

Electronic and magnetic properties of substitutional Mn clusters in (Ga,Mn)As

Hannes Raebiger,¹ Andrés Ayuela,² and J. von Boehm¹¹ COMP/Laboratory of Physics, Helsinki University of Technology, POB 1100, 02015 HUT, Finland.² Donostia International Physics Centre (DIPC), POB 1072, 20018 San Sebastian, Spain

(Dated: October 29, 2018)

The magnetization and hole distribution of Mn clusters in (Ga,Mn)As are investigated by all-electron total energy calculations using the projector augmented wave method within the density-functional formalism. It is found that the energetically most favorable clusters consist of Mn atoms surrounding one center As atom. As the Mn cluster grows the hole band at the Fermi level splits increasingly and the hole distribution gets increasingly localized at the center As atom. The hole distribution at large distances from the cluster does not depend significantly on the cluster size. As a consequence, the spin-flip energy differences of distant clusters are essentially independent of the cluster size. The Curie temperature T_C is estimated directly from these spin-flip energies in the mean field approximation. When clusters are present estimated T_C values are around 250 K independent of Mn concentration whereas for a uniform Mn distribution we estimate a T_C of about 600 K.

PACS numbers: 75.50.Pp; 85.75.-d

I. INTRODUCTION

In the diluted magnetic semiconductor (Ga,Mn)As the Mn atoms substituting Ga ones act as acceptors that simultaneously provide both local magnetic moments and spin-polarized p - d -type delocalized holes (according to a simple model one hole per Mn atom) which are generally believed to mediate the ferromagnetic coupling [1, 2, 3, 4, 5, 6, 7, 8, 9, 10, 11, 12]. This unique feature where magnetism is clearly intertwined with semiconductor properties makes (Ga,Mn)As a particularly attractive material both for basic research and spintronics applications. The Curie temperature (T_C) has been found to depend directly on the delocalized hole concentration [3, 4, 13, 14, 15, 16, 17, 18]. It has also been found that annealing of the molecular beam epitaxially grown (Ga,Mn)As removes Mn interstitial donors which increases delocalized hole concentration and consequently T_C [16, 19, 20]. The disorder of the Mn atoms either increases T_C further for lower Mn concentrations [21, 22, 23, 24] or decreases T_C [25]. Another mechanism which affects hole concentration (decreasingly) is the donation of electrons by the As antisite defects in the as-grown (Ga,Mn)As [14, 26, 27, 28, 29, 30].

However, an additional mechanism which surely affects magnetic coupling and the related hole distribution as well as T_C is the clustering of Mn atoms. $\text{Mn}_{\text{Ga}}\text{-Mn}_{\text{Ga}}$ dimer clusters (denoted henceforth by Mn_2 and called “dimer”) and Mn_{Ga} - interstitial Mn complexes have been found in as-grown (Ga,Mn)As samples from cross-sectional scanning tunneling microscopy images [31]. Some of these Mn_{Ga} - interstitial Mn complexes may disappear during annealing [20], but complexes where the interstitial Mn is bound to substitutional Mn clusters can be very stable [32]. The presence of Mn_2 -clusters is natural because for a characteristic Mn

concentration of $x = 5\%$ and assuming a random Mn distribution the probability that a Mn atom belongs to a cluster is $1 - 0.95^{12} \approx 0.46$. Structural evolution during post-growth annealing can lead to further clustering [14, 19, 33] but no precipitation has been found [33]. Recently several *first-principles* calculations based on the density-functional-theory have been performed to study the Mn clustering and the related changes in magnetism [25, 32, 34, 35, 36, 37, 38]. The general outcome of these calculations may be summarized as follows. Substitutional Mn clustering in (Ga,Mn)As is energetically favorable up to Mn_3 - or Mn_4 -clusters [34, 38]. Large magnetic moments are formed at the Mn clusters in (Ga,Mn)As [36, 37] [see also Ref. [35] for the case (Ga,Mn)N]. At the same time the p - d hole distribution grows significantly at the Mn clusters reducing the relative amount of delocalized holes available for the long range coupling of the magnetic moments of the Mn clusters [36, 38]. Interstitial Mn is also found to form a stable complex with Mn_2 [32].

The aim of this Paper is to study theoretically the electronic and magnetic properties of substitutional Mn clusters in (Ga,Mn)As paying special attention to the hole mediated magnetic coupling between the magnetic moments of the Mn clusters using *first-principles* methods. We limit ourselves solely to substitutional Mn clusters; interstitial Mn, As antisite or other possible point defects are not considered although they may influence the physics of (Ga,Mn)As [14, 26, 27, 28, 29, 30, 32]. The Paper is organized as follows. The computational methods are presented in Sec. II, the results for single substitutional Mn impurity, Mn cluster formation and magnetic coupling including discussion are presented in Sec. III, and the conclusions are drawn in Sec. IV.

Spin-polarized total energy supercell calculations based on the density-functional-theory are performed for (Ga,Mn)As. The projector augmented-wave method together with the generalized gradient approximation (GGA-PW91) for exchange-correlation as implemented in the VASP code is employed [39, 40, 41]. The projector augmented wave method has the advantage that it is basically an all-electron method but nevertheless almost as fast as the usual plane-wave pseudopotential method. However, a slight limitation of the VASP implementation is the fact that the core states are kept fixed. The projector augmented-wave potentials and the pseudopotentials for plane waves provided in the VASP package were compared with an all-electron full-potential linearized augmented-plane-wave calculation by performing calculations for MnAs (a crystal having the GaAs structure but Mn substituting Ga). The projector augmented-wave calculation was found to agree closely with the linearized augmented-plane-wave calculation but to differ both quantitatively and qualitatively from the plane-wave pseudopotential calculation [36].

In our calculations plane-waves up to the 275 eV cut-off value are included; total energy in several test systems change less than 1 meV as the cut-off value is increased from 275 to 300 eV or from 275 to 325 eV. Since (Ga,Mn)As is a half-metal a dense k-mesh is needed. The Brillouin zone integrations are done using the linear tetrahedron method with Bloechl corrections [40]. The Monkhorst-Pack $(0.14 \text{ \AA}^{-1})^3$ mesh including the Γ -point was found sufficiently accurate for the Brillouin zone sampling [36] and is used in this study. One or two Mn clusters (comprising of up to 5 Mn atoms substituting Ga sites) are included in supercells of 64, 96 or 128 atoms, corresponding to $2 \times 2 \times 2$, $2 \times 2 \times 3$ and $2 \times 2 \times 4$ cubic zincblende unit cells, respectively. Thus, the Mn concentration in our calculations varies in the experimentally relevant range $[\text{Mn}] = 1.6 \dots 7.8 \%$. Various Mn cluster distributions and different spin alignments (e.g. $\uparrow\uparrow$ vs. $\uparrow\downarrow$) are studied. Since relaxation effects were found negligible in the 64 atom supercell calculations, only unrelaxed lattice positions with the fixed experimental lattice constant $a = 5.65 \text{ \AA}$ are used for larger supercells. The orbital decomposition analysis is performed using the standard methods implemented in the VASP code [40]. The self interaction error and the spin-orbit interactions are expected to be small for (Ga,Mn)As [42, 43, 44, 45] and thus neglected in our calculations.

III. RESULTS AND DISCUSSION

A. Mn_{Ga} impurity in the dilute limit

The calculated density of states (DOS) for a uniform [46] substitutional Mn distribution in our dilute limit of $x = 1.6 \%$ (or one substitutional Mn atom in

the 128 atom supercell) is shown in Fig. 1 for reference. The formation of the DOS may be followed using the simple branching diagram of Fig. 1 (a). The removal of a Ga atom creates a vacancy (V_{Ga}) acting as a shallow triple acceptor. The six-fold degenerate p -type t_2 -level of the V_{Ga} is occupied by three electrons [47, 48]. When the Mn atom ($3d^5 4s^2$) is placed to the V_{Ga} , the V_{Ga} p states and the Mn d states hybridize into the $t_{b\uparrow}$ & $t_{b\downarrow}$ bonding states, the e_{\uparrow} & e_{\downarrow} states, and the $t_{a\uparrow}$ & $t_{a\downarrow}$ antibonding states. The three electrons from the V_{Ga} and the seven electrons from the Mn atom occupy the three $t_{b\uparrow}$ bonding states, the two e_{\uparrow} states, the three $t_{b\downarrow}$ bonding states, and two of the three $t_{a\uparrow}$ antibonding states leaving one unoccupied state (Fig. 1 (a)). The bands and the DOS are subsequently formed as shown in Fig. 1 (b). The most important feature of the DOS is the single hump in the majority spin (\uparrow) channel at the Fermi level (E_F) which makes (Mn,Ga)As a half-metal (Figs 1 (b) and (c)). As discussed above, the hump is formed mainly from the $t_{a\uparrow}$ antibonding states (Fig. 1 (a)). Each Mn atom contributes one hole state in the unoccupied part of the hump as well as the net magnetic moment of $4\mu_B$ [two e_{\uparrow} and two $t_{a\uparrow}$ electrons, see Fig. 1 (a)] (μ_B is the Bohr magneton). Our calculated DOS in Fig. 1 agrees closely with several other independent calculations [24, 45, 49, 50, 51, 52, 53].

The spin-polarized hole density of the hump consists mainly of the Mn d part localized around the Mn atoms and the As p part that is *delocalized* around the As atoms. This delocalization can be seen in the calculated As p projection of the hole distribution shown in Fig. 2 (the average number of p holes at the As atoms belonging to each coordination shell measured from the closest Mn site is given; for comparison the number of holes at the Mn site is about 0.13). The peaks at the distances of 2.4 and 6.2 \AA belong to the nearest and third nearest As coordination shells. Otherwise the p hole distribution appears to be quite even. The p hole distribution does not change significantly when the Mn concentration is changed (cf. the solid and dotted lines in Fig. 2 corresponding to the Mn concentrations of 1.6 and 2.1 %, respectively).

B. Formation of Mn clusters

The energetically most important calculated Mn cluster configurations are shown in Fig. 3. The supercells used are chosen such that the Mn concentration remains the same $x = 6.3 \%$. However, in the case of five substitutional Mn atoms in the supercell a slightly higher concentration of 7.8 % is allowed due to the computational limitations. For the cases of 2-4 Mn atoms in the supercell the configuration where the Mn atoms share the *same neighbouring* As site is always found to be energetically most favorable (see the upper left-hand corners in Figs 3 (a) - (c)). Also, it is energetically favorable to form one cluster from two separate components in all cases shown in Figs 3 (a) - (c). In the case of five Mn

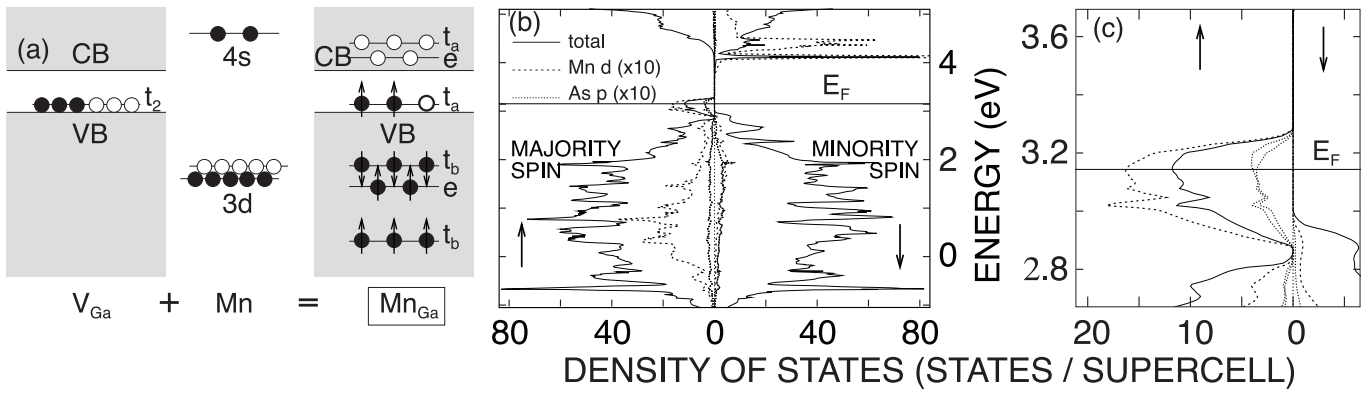


FIG. 1: The calculated density of states (DOS) for the Mn concentration of $x = 1.6\%$. (a) Branching diagram for a substitutional Mn atom. The states of the substitutional Mn atom are formed via the hybridization of the $V_{\text{Ga}} t_2$ and Mn $3d$ states. (b) DOS. E_F denotes the Fermi level. (c) The magnification of the DOS around E_F .

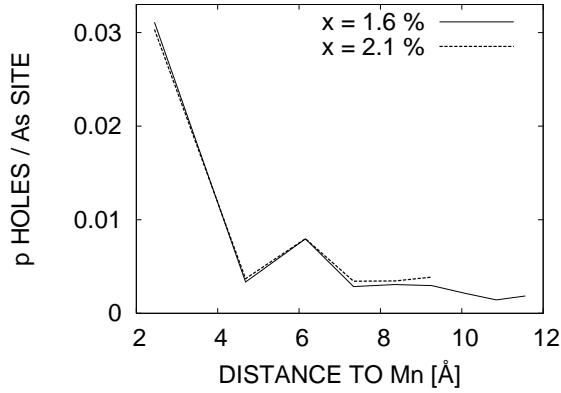


FIG. 2: The calculated As p hole distribution. The average number of p holes per As site at each As coordination cell is given. The numbers are obtained by integration from the orbital decomposition. Note that the orbital decomposition as well as the choice of the integration volume are not unambiguous. Nevertheless, the relative magnitudes are directly comparable.

atoms in the supercell the energetically most favorable configuration is obtained by attaching the fifth Mn atom to the stable tetramer [Fig. 3 (d)]. The energies needed to separate single clusters into two components (or the binding energies for the components) are shown graphically in Fig. 3 as black horizontal bars which contain also the corresponding energy values in the units of meV. In all these cases the ferromagnetic order is the stablest magnetic phase. By using the above binding energies we have calculated the heats of reaction for the cluster formation and found that the optimal cluster sizes are tetramers being slightly more favorable than the trimers [38]. Our calculation showing that clustering is energetically favorable is in agreement with the experimental result that Mn_2 clusters appear already in the as-grown (Ga,Mn)As samples [31]. Further clustering is expected during post-

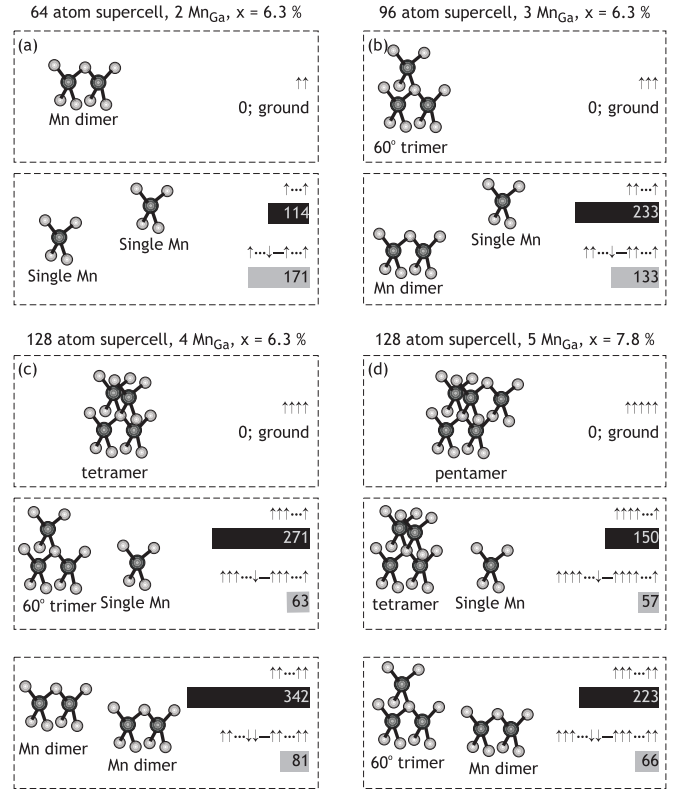


FIG. 3: Calculated Mn cluster configurations and total energies. The dark and gray balls denote the Mn and As atoms, respectively. Separated components are placed at the maximum distance available. All the black horizontal bars show the (ferromagnetic) separation (or binding) energies; the corresponding values are given in the units of meV in the black bars. The gray horizontal bars with the arrow diagrams show the spin-flip energies; the corresponding values are given in the units of meV inside the gray bars. All the black and gray horizontal bars are drawn in the same scale.

C. Effects of clustering

The dilute-limit majority-spin hump at the Fermi energy E_F in Fig. 1 (c) is found to split when Mn clusters are formed, and new narrower unoccupied bands appear in the gap. This is shown for the Mn monomer, dimer, trimer, and tetramer systems at the constant Mn concentration of $x = 6.3\%$ in Fig. 4. At the same time the hole density grows at the As atom which is situated in the center of the Mn cluster. This was shown for the Mn dimer in Ref. [36] and a similar splitting was also found in Ref. [37]. The increasing localization at the center As atom is reflected in the increasing separation and size of the split-off part of the hump in Fig. 4. The As p -projection in the split-off part of the hole DOS is seen to increase in relation to the Mn d -projection in Fig. 4 and even to exceed the Mn d projection in the cases of the Mn trimer and tetramer [Figs 4 (c) and (d)].

The integrated numbers of the Mn d holes at the cluster Mn atoms and the As p holes at the center As atom of the clusters are given in Table I. The results in Table I clearly show that the number of the As p holes grows relatively faster than the number of the Mn d holes as the cluster size increases. In the case of the pentamer, the fifth Mn atom lies outside the tetramer and, in addition to the center As atom inside the tetramer, there are two equivalent As atoms between the fifth Mn atom and the tetramer [Fig. 3 (d)]. In this case the holes in the tetramer part remain intact whereas the numbers of the Mn d and As p holes are seen to grow at the additional fifth Mn atom and the two associated As atoms, respectively (see the last line of Table I). We expect that an additional sixth Mn atom would cause further hole growth at the new center-As-atom.

The As p component of the spin-polarized hole density as a function of the distance to the closest Mn atom is shown in Fig. 5 for several different cluster sizes. At short distances $r < 7 \text{ \AA}$ to the closest Mn atom of the cluster, the hole concentration increases with increasing number of Mn atoms. However, for larger distances $r > 7 \text{ \AA}$ the hole concentrations approach the same curve. Therefore, the long-distance magnetic coupling between the Mn clusters depends only on their mutual distance, not on the size of the cluster.

In addition to the different ferromagnetic cluster configurations above also various other magnetic alignments were considered. As mentioned above, the ferromagnetic alignment is always energetically most stable. The intra-cluster spin-flip energy is relatively high for the Mn dimer: 211 meV [36] and significantly higher inside the larger clusters, typically 300 meV and more. The spin flip energy of a distant component describes the stability of the long range ferromagnetic state and may also be used estimating T_C as will be discussed shortly. The calculated spin-flip energies Δ for the spin-flips of dis-

TABLE I: Holes inside the Mn cluster. The numbers of the Mn d holes at the cluster Mn atoms and the As p holes at the As atom which is the center of the Mn cluster are given. The numbers are obtained by integration from the orbital decomposition. Although the orbital decomposition as well as the choice of the integration volume are not unambiguous the given average numbers of p holes are directly comparable.

System	Mn d holes	As p holes	x (%)
single Mn	0.13	0.03	6.3
dimer	0.17	0.11	6.3
trimer	0.19	0.19	6.3
tetramer	0.21	0.29	6.3
pentamer	0.21 ($\times 4$)	0.28 ($\times 1$)	7.8
	0.19 ($\times 1$)	0.10 ($\times 2$)	

tant Mn atoms or entire clusters are given in Table II as well as in Fig. 3 as gray horizontal bars containing also the corresponding energy values in the units of meV. The Mn concentrations x in Table II are chosen such that the closest Mn-Mn distance is constant (10.6 \AA) except for the first row where the distance is 13.8 \AA . The calculated Δ values vary relatively little, between 57 and 81 meV. This variation in the Δ values exhibits no evident trend; e.g. by looking at configurations with one cluster fixed, an increase of the second cluster size leads to either increase or decrease of the Δ value. These fluctuations may be caused by e.g. directional effects [54, 55]. This shows clearly that new Mn atoms in the clusters promote the holes mainly to the center As atom of the cluster and thus do not increase the delocalized hole concentration mediating the ferromagnetic cluster-cluster coupling.

The following expression based on the mean-field approximation may be used to roughly estimate T_C [53, 56, 57]

$$T_C = \frac{2}{3k_B} \frac{\Delta}{N}, \quad (1)$$

where Δ is the energy difference between the spinglass and ferromagnetic arrangements in the supercell, and N denotes the number of the magnetic particles in the supercell. However, we choose to calculate Δ as the difference between the anti-parallel and parallel arrangements which is known to be a good approximation [56, 57]. We treat the Mn clusters as single magnetic particles, and calculate Δ from the cluster-cluster spin-flip energies. The number of Mn clusters in the supercell is always fixed to $N = 2$.

First, we consider the simple antiferromagnetic-ferromagnetic case. Using Eq.(1) we estimate that for a uniform Mn monomer distribution T_C is 220 K for $x = 3.1\%$ (Table II) and 620 K for $x = 6.3\%$ [36]. The increase of T_C from 220 to 620 K is mainly due to the decrease of the Mn-Mn distance from 13.8 to 9.8 \AA . If at $x = 6.3\%$ the Mn atoms were distributed randomly at the Ga sites, about $1 - 0.937^{12} = 54\%$ of the Mn atoms would belong to clusters. Therefore it is of some interest to

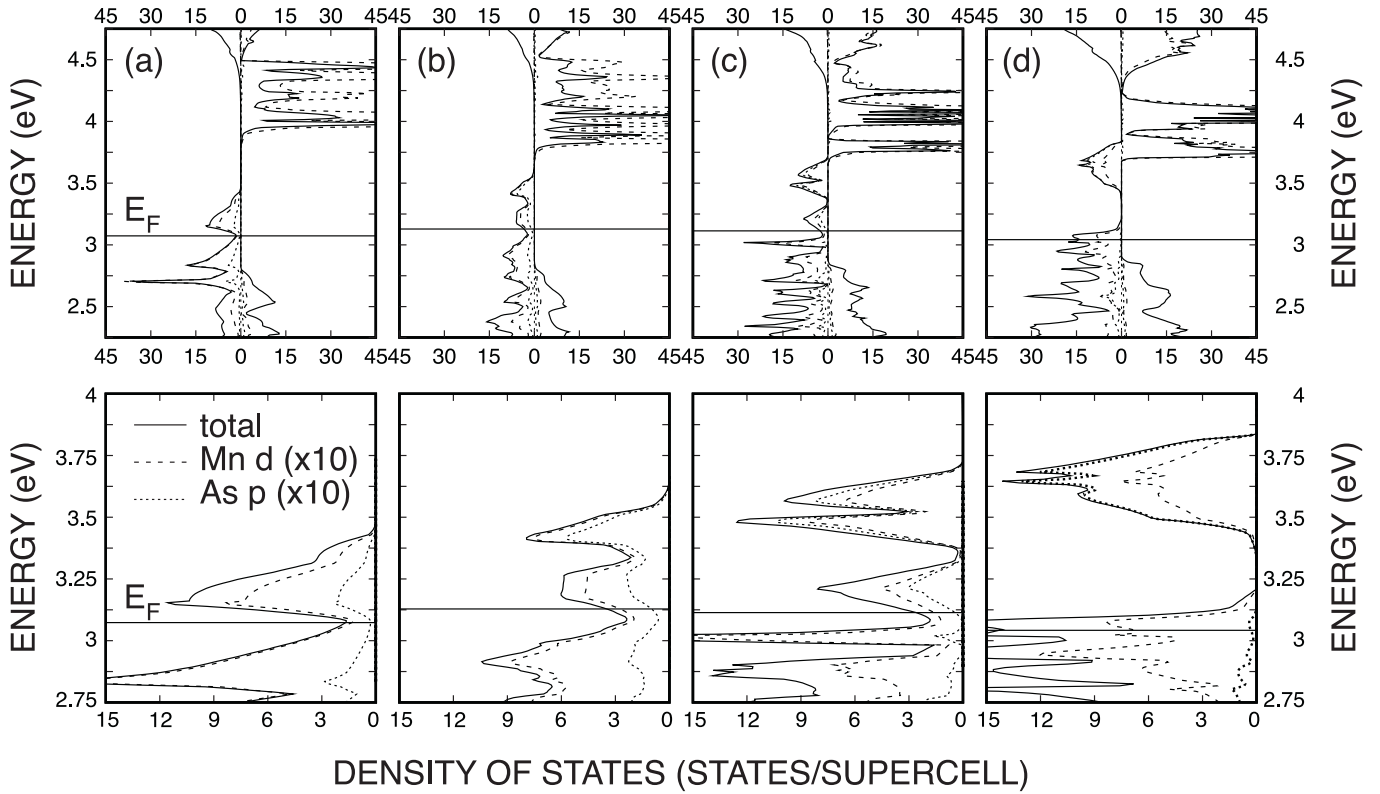


FIG. 4: Densities of states (DOSs) around the band gap (upper figures) and the magnifications of the majority spin DOSs around the Fermi energy (E_F) (lower figures). Figures (a), (b), (c), and (d) give the DOSs for the Mn monomer, dimer, trimer, and tetramer, respectively for the Mn density of $x = 6.3\%$.

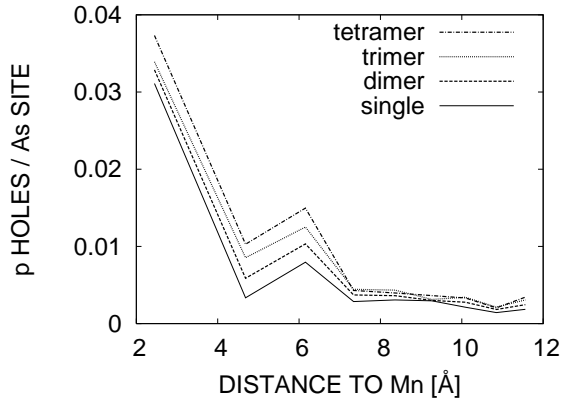


FIG. 5: The calculated As p hole distribution for different cluster sizes. For further information see the caption of Fig. 2.

compare the uniform Mn-dimer distribution at $x = 6.3\%$ (all Mn atoms belong to dimers) with the uniform Mn monomer distribution at $x = 6.3\%$. The dimerization reduces T_C from 620 K to 313 K (Table II). A similar dramatic decrease of T_C is found at $x = 12.5\%$ from a uniform Mn distribution to the corresponding Mn_4 cluster distribution in Ref. [37], but at $x = 6.3\%$ a slight

increase in T_C is found from a uniform Mn distribution to the corresponding dimer distribution. In Ref. [25] it was concluded quite generally that clustering decreases T_C , which is in agreement with our findings.

We follow the same procedure as above to estimate T_C from Eq.(1) for further cluster distributions. The estimated T_C values are given in Table II where the Mn concentrations x are chosen such that the closest Mn-Mn distance is always 10.6 \AA (except for the Mn_1+Mn_1 case). As noted above Δ does not depend significantly on the Mn concentration and therefore neither does T_C : the calculated T_C values vary between 220 and 313 K (Table II). This may be related to the fact that the average As p hole distribution at large distances ($> 7 \text{\AA}$) is almost independent of the number of Mn atoms in each cluster. Thus, as long as the distance between clusters is kept constant, T_C does not vary significantly though the number of Mn atoms in the clusters is changed.

In the mean field approximation, T_C is proportional to Δ/N (Eq.(1)). During clustering, Δ may be expected to decrease exponentially with respect to the growing cluster-cluster distance while the number of clusters N in the denominator decreases much more slowly. Thus, as already noted above for the uniform dimer distribution, clustering decreases T_C significantly.

With the present high quality (Ga,Mn)As samples

TABLE II: Spin-flip total energy differences between two substitutional Mn clusters. Δ is the energy difference between the system with one of the two clusters in anti-parallel spin state (A) with respect to the system with all spins ferromagnetically aligned (FM). The 128 atom supercell is used.

System	FM	A	Δ (meV)	T_C (K)	x (%)
Mn ₁ +Mn ₁	$\uparrow \cdots \uparrow$	$\uparrow \cdots \downarrow$	57	220	3.1
Mn ₂ +Mn ₁	$\uparrow\uparrow \cdots \uparrow$	$\uparrow\uparrow \cdots \downarrow$	73	282	4.7
Mn ₃ +Mn ₁	$\uparrow\uparrow\uparrow \cdots \uparrow$	$\uparrow\uparrow\uparrow \cdots \downarrow$	63	244	6.3
Mn ₂ +Mn ₂	$\uparrow\uparrow \cdots \uparrow\uparrow$	$\uparrow\uparrow \cdots \downarrow\downarrow$	81	313	6.3
Mn ₄ +Mn ₁	$\uparrow\uparrow\uparrow\uparrow \cdots \uparrow$	$\uparrow\uparrow\uparrow\uparrow \cdots \downarrow$	57	220	7.8
Mn ₃ +Mn ₂	$\uparrow\uparrow\uparrow \cdots \uparrow\uparrow$	$\uparrow\uparrow\uparrow \cdots \downarrow\downarrow$	66	255	7.8

where the amount of the harmful interstitial Mn and As_{Ga} defects has been minimized one achieves T_C 's in the range of 159-173 K [20, 58]. The mean field approximation used here may be expected to give an upper limit in estimating T_C . The obtained estimates ranging between 220 and 313 K in the case of clustering (Table II) agree quite reasonably with these best experimental values. This is consistent with the fact that real samples contain clusters [31] which, as was shown above, can reduce T_C strongly.

IV. CONCLUSION

Substitutional Mn clustering in the diluted (Ga,Mn)As magnetic semiconductor is studied by means of spin-polarized all-electron density-functional calculations. The clustering is an important factor in the typical Mn concentration range from 1 to 10 % because already in the case of purely random Mn distribution the probability that a Mn atom belongs to a cluster varies correspondingly from 0.1 to 0.7. Furthermore, our calculations show that cluster formation is energetically favorable. The en-

ergetically most stable clusters are found to consist of Mn atoms that surround symmetrically the center As atom. The spin-polarized hole distribution is found to get increasingly localized at this center As atom and the majority spin DOS hump at the Fermi level to split when the cluster size increases from Mn₁ to Mn₄. At the same time the hole density outside the cluster depends relatively little on the number of Mn atoms in the cluster, especially at larger distances ($> 1.2 \times$ lattice constant). This implies that the long range ferromagnetic coupling between two Mn clusters depends relatively little on the number of Mn atoms in the clusters. Our calculated spin-flip energies confirm this expectation. Using these spin-flip energies and the mean field approximation we estimate Curie temperatures around 250 K for the various studied cluster distributions independently of the Mn concentration. In contrast, we estimate for a uniform Mn monomer distribution at $x = 6.3$ % a high value of 620 K. The best present (Ga,Mn)As samples achieve Curie temperatures of 159-173 K. Therefore, our estimated Curie temperature values are consistent with the fact that the (Ga,Mn)As samples are hampered by the clustering effect.

V. ACKNOWLEDGMENTS

This work has been supported by the Academy of Finland through the Center of Excellence Program (2000-2005). A.A. acknowledges the financing of the Basque Government by the ETORTEK program called NANOMAT. The authors thank Acad. Prof. R. M. Nieminen, Prof. K. Saarinen, Prof. M. J. Puska, Dr. M. Alava, Mr. F. Tuomisto and Mr. T. Hynninen for many valuable discussions. We acknowledge the generous computing resources of the Center for Scientific Computing (CSC).

-
- [1] H. Ohno, A. Shen, F. Matsukura, A. Oiwa, A. Endo, S. Katsumoto, and Y. Iye, *Appl. Phys. Lett.* **69**, 363 (1996).
 - [2] F. Matsukura, H. Ohno, A. Shen, and Y. Sugawara, *Phys. Rev. B* **57**, R2037 (1998).
 - [3] H. Ohno, *Science* **281**, 951 (1998).
 - [4] H. Ohno, *J. Magn. Magn. Mater.* **200**, 110 (1999).
 - [5] J. Szczytko, W. Mac, A. Twardowski, F. Matsukura, and H. Ohno, *Phys. Rev. B* **59**, 12935 (1999).
 - [6] B. Beschoten, P. A. Crowell, I. Malajovich, D. D. Awschalom, F. Matsukura, A. Shen, and H. Ohno, *Phys. Rev. Lett.* **83**, 3073 (1999).
 - [7] T. Dietl, H. Ohno, F. Matsukura, J. Cibert, and D. Ferrand, *Science* **287**, 1019 (2000).
 - [8] H. Ohno and F. Matsukura, *Solid State Commun.* **117**, 179 (2001).
 - [9] H. Akinaga and H. Ohno, *IEEE Trans. Nanotechn.* **1**, 19 (2002).
 - [10] H. Képa, Le Van Khoi, C. M. Brown, M. Sawicki, J. K. Furdyna, T. M. Giebultowicz, and T. Dietl, *Phys. Rev. Lett.* **91**, 087205 (2003).
 - [11] J. M. D. Coey and S. Sanvito, *J. Phys. D: Appl. Phys.* **37**, 988 (2004).
 - [12] T. Dietl, in *Proceedings of 27th International Conference on Physics of Semiconductors, Flagstaff, Arizona, USA, July 2004*, edited by J. Mendez, AIP Proceedings, cond-mat/0408561 2004 (unpublished).
 - [13] Y. Satoh, N. Inoue, Y. Nishikawa, and J. Yoshino, in *3rd Symposium on Physics and Application of Spin-Related Phenomena in Semiconductors, Senadai, Japan, November 1997*, edited by H. Ohno, Y. Oka, and J. Yoshino, p. 23.
 - [14] S. Potashnik, K. Ku, S. Chun, J. Berry, N. Samarth, and P. Schiffer, *Appl. Phys. Lett.* **79**, 1495 (2001).

- [15] K. Edmonds, K. Wang, R. Campion, A. Neumann, N. Farley, B. Callagher, and C. Foxon, *Appl. Phys. Lett.* **81**, 4991 (2002).
- [16] K. M. Yu, W. Walukiewicz, T. Wojtowicz, W. L. Lim, X. Liu, U. Bindley, M. Dobrowolska, and J. K. Furdyna, *Phys. Rev. B* **68**, 041308 (R) (2003).
- [17] K. C. Ku, S. J. Potashnik, R. F. Wang, S. H. Chun, P. Schiffer, N. Samarth, M. J. Seong, A. Mascarenhas, E. Johnston-Halperin, R. C. Myers, A. C. Gossard, and D. D. Awschalom, *Appl. Phys. Lett.* **82**, 2302 (2003).
- [18] B. S. Sørensen, P. E. Lindelof, J. Sadowski, R. Mathieu, and P. Svedlindh, *Appl. Phys. Lett.* **82**, 2287 (2003).
- [19] K. M. Yu, W. Walukiewicz, T. Wojtowicz, I. Kuryliszyn, X. Liu, Y. Sasaki, and J. K. Furdyna, *Phys. Rev. B* **65**, 201303 (R) (2002).
- [20] K. W. Edmonds, P. Boguslawski, K. Y. Wang, R. P. Campion, S. N. Novikov, N. R. S. Farley, B. L. Gallagher, C. T. Foxon, M. Sawicki, T. Dietl, M. Buongiorno Nardelli, and J. Bernholc, *Phys. Rev. Lett.* **92**, 037201 (2004).
- [21] M. Berciu and R. N. Bhatt, *Phys. Rev. Lett.* **87**, 107203 (2001); C. Timm, F. Schäfer, and F. von Oppen, *Phys. Rev. Lett.* **90**, 029701 (2003); M. Berciu and R. N. Bhatt, *Phys. Rev. Lett.* **90**, 029702 (2003).
- [22] A. L. Chudnovskiy and D. Pfannkuche, *Phys. Rev. B* **65**, 165216 (2002).
- [23] A. Kaminski and S. Das Sarma, *Phys. Rev. Lett.* **88**, 247202 (2002).
- [24] L. M. Sandratskii, P. Bruno, and J. Kudrnovsky, *Phys. Rev. B* **69**, 195203 (2004).
- [25] J. L. Xu, M. van Schilfgaarde, and G. D. Samolyuk, *Phys. Rev. Lett.* **94**, 097201 (2005).
- [26] B. Grandidier, J. P. Nys, C. Delerue, D. Stiévenard, Y. Higo, and M. Tanaka, *Appl. Phys. Lett.* **77**, 4001 (2000).
- [27] S. Sanvito and N. A. Hill, *Appl. Phys. Lett.* **78**, 3493 (2001).
- [28] P. A. Korzhavyi, I. A. Abrikosov, E. A. Smirnova, L. Bergqvist, P. Mohn, R. Mathieu, P. Svedlindh, J. Sadowski, E. I. Isaev, Yu. Kh. Vekilov, and O. Eriksson, *Phys. Rev. Lett.* **88**, 187202 (2002).
- [29] J. Kudrnovský, I. Turek, V. Drchal, F. Máca, P. Weinberger, and P. Bruno, *Phys. Rev. B* **69**, 115208 (2004).
- [30] F. Tuomisto, K. Pennanen, K. Saarinen and J. Sadowski, *Phys. Rev. Lett.* **93**, 055505 (2004).
- [31] J. M. Sullivan, G. I. Boishin, L. J. Whitman, A. T. Hanbicki, B. T. Jonker, and S. C. Erwin, *Phys. Rev. B* **68**, 235324 (2003).
- [32] P. Mahadevan and A. Zunger, *Phys. Rev. B* **68**, 075202 (2003).
- [33] T. Hayashi, Y. Hashimoto, S. Katsumoto, and Y. Iye, *Appl. Phys. Lett.* **78**, 1691 (2001).
- [34] M. van Schilfgaarde and O. N. Mryasov, *Phys. Rev. B* **63**, 233205 (2001).
- [35] B. K. Rao and P. Jena, *Phys. Rev. Lett.* **89**, 185504 (2002).
- [36] H. Raebiger, A. Ayuela and R. M. Nieminen, *J. Phys.: Condens. Matter* **16**, L457 (2004).
- [37] L. M. Sandratskii and P. Bruno, *J. Phys.: Condens. Matter* **16**, L523 (2004).
- [38] H. Raebiger, A. Ayuela, J. von Boehm, and R. M. Nieminen, *J. Magn. Magn. Mater.* **290-291P2**, 1398 (2005).
- [39] J. P. Perdew and Y. Wang, *Phys. Rev. B* **45**, 13244 (1992); and references therein.
- [40] G. Kresse and J. Furthmüller, *Phys. Rev. B* **54**, 11169 (1996); G. Kresse and J. Furthmüller, *VASP the Guide* (Vienna University of Technology, Vienna, 1999) [<http://tph.tuwien.ac.at/~vasp/guide/vasp.html>]
- [41] G. Kresse and D. Joubert, *Phys. Rev. B* **59**, 1758 (1999).
- [42] A. J. R. da Silva, A. Fazzio, R. R. dos Santos, and L. E. Oliveira, *J. Phys.: Condens. Matter* **16**, 8243 (2004).
- [43] J. P. Perdew and A. Zunger, *Phys. Rev. B* **23**, 5048 (1981).
- [44] A. Filippetti, N. A. Spaldin, and S. Sanvito, *Chem. Phys.* **309**, 59 (2004).
- [45] M. Wierzbowska, D. Sánchez-Portal, and S. Sanvito, *Phys. Rev. B* **70**, 235209 (2004).
- [46] In this Paper the uniform Mn distribution means a regular, periodic Mn sublattice with no clustering, calculated within the supercell approach. This does not correspond to the homogeneous disorder in the coherent potential approximation calculations.
- [47] K. Laasonen, R. M. Nieminen, and M. J. Puska, *Phys. Rev. B* **45**, 4122 (1992).
- [48] U. Scherz and M. Scheffler, in *Imperfections in III/V Materials, Semiconductors and Semimetals* **38**, p. 1 (1992).
- [49] S. Sanvito, P. Ordejón, and N. A. Hill, *Phys. Rev. B* **63**, 165206 (2001).
- [50] K. Sato and H. Katayama-Yoshida, *Jpn. J. Appl. Phys.* **40**, L485 (2001).
- [51] E. Kulatov, H. Nakayama, H. Mariette, H. Ohta, and Yu. A. Uspenskii, *Phys. Rev. B* **66**, 045203 (2002).
- [52] L. Bergqvist, P. A. Korzhavyi, B. Sanyal, S. Mirbt, I. A. Abrikosov, L. Nordström, E. A. Smirnova, P. Mohn, P. Svedlindh, and O. Eriksson, *Phys. Rev. B* **67**, 205201 (2003).
- [53] K. Sato, P. H. Dederichs, and H. Katayama-Yoshida, *Europhys. Lett.* **61**, 403 (2003).
- [54] B. Sanyal, O. Bengone, and S. Mirbt, *Phys. Rev. B* **68**, 205210 (2003).
- [55] P. Mahadevan, A. Zunger, and D. D. Sarma, *Phys. Rev. Lett.* **93**, 177201 (2004).
- [56] Ph. Kurz, G. Bihlmayer, and S. Blügel, *J. Phys.: Condens. Matter* **14**, 6353 (2002).
- [57] I. Turek, J. Kudrnovský, G. Bihlmayer, and S. Blügel, *J. Phys.: Condens. Matter* **15**, 2771 (2003).
- [58] K. Y. Wang, R. P. Campion, K. W. Edmonds, M. Sawicki, T. Dietl, C. T. Foxon, and B. L. Gallagher in *Proceedings of 27th International Conference on Physics of Semiconductors, Flagstaff, Arizona, USA, July 2004*, edited by J. Mendez, AIP Proceedings, cond-mat/0411475, 2004 (unpublished).